International Journal of Heat and Fluid Flow 30 (2009) 452–461

Contents lists available at ScienceDirect

International Journal of Heat and Fluid Flow

journal homepage: www.elsevier.com/locate/ijhff

Eulerian-Eulerian prediction of dilute turbulent gas-particle flow in a backward-facing step

Aldo Benavides [a,*], Berend van Wachem [b]

[a] Applied Mechanics, Chalmers University of Technology, SE-41296 Gothenburg, Sweden
[b] Department of Mechanical Engineering, Imperial College London, SW7 2AZ, United Kingdom

ARTICLE INFO

Article history:
Received 29 September 2008
Received in revised form 10 February 2009
Accepted 14 February 2009
Available online 29 March 2009

Keywords:
Gas-particle flow
Eulerian approach
Kinetic theory of granular flow (KTGF)
Turbulence modulation

ABSTRACT

A numerical study of turbulent gas-particle flow in a two-dimensional, vertically oriented backward-facing step is compared with literature data. The dispersed phase is modeled by an Eulerian approach based upon the kinetic theory of granular flow (KTGF) including models for describing the dispersed phase interactions with the continuous phase. The modeling of turbulent motion within the dispersed phase and the correlation between gas and particle velocity fluctuations are discussed. In addition, closure relations for the dispersed phase are extended to incorporate interstitial fluid effects. The continuous phase turbulence is modeled by a $k-\epsilon$ model. This work demonstrates that treatment of turbulent characteristics is a key element in predicting the dispersed phase mean motion and turbulence modulation in the continuous phase. The derived models are implemented in a commercial code and simulation results are compared with benchmark experimental data for three particle classes with distinctive particle Stokes number, particle Reynolds number and mass-loading. In general, reasonable predictions are achieved.

1. Introduction

Knowledge of the hydrodynamics of turbulent gas-particle flows has a great importance for the successful design and determination of optimum operating conditions of numerous industrial applications, e.g., cyclone separators, fluidized beds, dust collectors, and pulverized-coal combustors, to name a few. These systems exhibit complex flow dynamics and interaction of flow components. The particle response in the presence of an interstitial fluid and gas turbulence modulation by particles are two topics that have stimulated research work in recent years (Fessler and Eaton, 1999; Lun, 2000; Zhang and Reese, 2003; Hadinoto and Curtis, 2004).

The presence of particles in turbulent flows may modify the turbulence structure of the continuous gas-phase as a result of momentum transfer from the particles. Elgobashi (1994) identifies a range of particulate phase volume fraction between 10^{-6} and 10^{-3} where particles can either augment or attenuate turbulence. Such degree of turbulence modification seems to correlate with both the particle Reynolds number and Stokes number. This is known as two-way coupling regime. Yu et al. (2004) report a numerical investigation of particle-laden turbulent flow over a backward facing step in which the gas-phase flow field is determined by LES and the motion of individual particles is traced throughout the flow domain (Lagrangian approach). However, their numerical investigation neglects the effect of particles on the carrier fluid flow, i.e., one-way-coupling is assumed, particle-particle interactions are not considered and particle-wall collisions are assumed to be perfectly elastic. Their research focuses on the dispersion of particles with different Stokes numbers, rather than turbulence modification by the particles.

The purpose of this paper is to perform a numerical investigation of a particle-laden backward-facing step with a turbulent channel flow inlet (Fig. 1) as it is described by Fessler and Eaton (1995), Fessler and Eaton (1999), for three particle sizes with particle Stokes number greater than unity. The modeling of the dispersed phase is accomplished by an Eulerian approach which treats the solids or particulate phase as a continuous medium with properties analogous to those of a fluid. Such technique involves the solution of a second set of Navier–Stokes-like equations in addition to those of the carrier (gas) phase. Furthermore, the significance of gas-particle interaction is reflected in the momentum and kinetic energy coupling terms via mean and fluctuating drag force, respectively.

Turbulence in the dispersed phase is modeled by a transport equation for the turbulent kinetic energy of the particles, or granular temperature. However, this modeling approach, directly derived from KTGF, does not generally consider the effect of gas-phase turbulence on the dispersed phase fluctuating motion (Lun et al., 1984; Gidaspow, 1994). A comprehensive gas-particle turbulence model derived in this paper accounts for such an important

* Corresponding author. Tel.: +46 31 772 5034.
E-mail address: benavide@chalmers.se (A. Benavides).

0142-727X/$ - see front matter © 2009 Elsevier Inc. All rights reserved.
doi:10.1016/j.ijheatfluidflow.2009.02.012

Nomenclature

C	correction coefficient
c	turbulence model constants
$\mathscr{D}$	dispersion coefficient
d	particle mean diameter
e	restitution coefficient
g	gravity
g_0	radial distribution function
h	channel width
H	step height
k	turbulent kinetic energy
ℓ	characteristic length-scale
P	mean pressure
$\mathscr{P}$	production term
R	Reynolds stress
Re_p	particle Reynolds number
S	rate of strain
$\mathscr{T}$	viscous stress
U	mean velocity
$\mathscr{U}$	characteristic velocity-scale
u	velocity fluctuation
$\overline{\bar{u}}$	averaged instantaneous velocity
$\overline{u_f^i u_s^j}$	fluid-particle correlation tensor
$\mathscr{X}$	mass-ratio
x	stream-wise coordinate
y	wall-normal coordinate

Greeks

β	drag function
Γ	conductivity
δ	Kronecker delta
ϵ	rate of dissipation
η	characteristic time ratio
Θ	granular temperature
κ	diffusivity
λ	bulk viscosity
μ	shear viscosity
ν	viscosity
ξ	Csanady parameter
Π	inter-phase energy exchange
ρ	density
σ	turbulence model constants
τ	characteristic time-scale
Φ	volume fraction

Superscripts

c	particle-collision property
i,j,l	index notation
t	turbulent quantity
0	single-phase

Subscripts

cl	center-line
d	related to drag or drift
f	gas or carrier phase
in	inlet
mfp	mean-free-path
r	relative slip
s	dispersed or particulate phase
sf	gas-particle interaction term

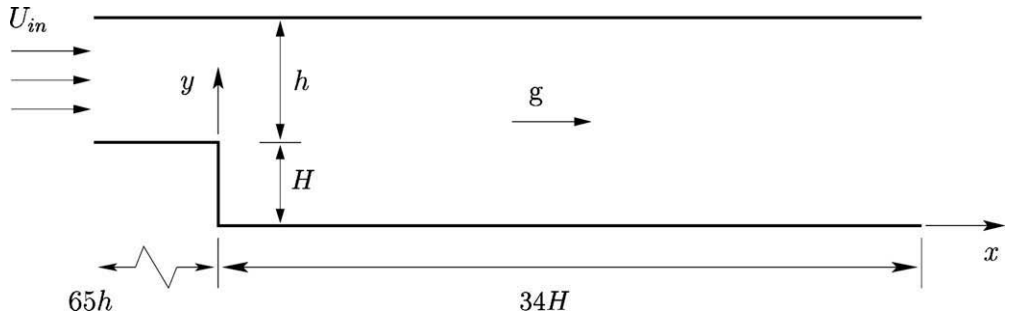

Fig. 1. Geometry of vertically oriented backward-facing step. The channel width (h) and step height (H) are 40 mm and 26.7 mm, respectively.

flow characteristic. The present work extends the use of KTGF to incorporate the effect of gas-particle interaction on the prediction of mean flow quantities.

2. Modeling

In an Eulerian model, the dispersed particle phase is treated as a fluid, in the same way as the carrier gas phase, so that a set of Favre-averaged conservation equations for the mass and momentum of both phases, turbulent kinetic energy and dissipation rate can be derived accordingly (Benavides and van Wachem, 2008). As a result, momentum and kinetic energy coupling terms arise in the transport equations due to the mean and fluctuating drag force contributions.

2.1. Dispersed phase

The Favre-averaged continuity equation is written as

$$\frac{\partial}{\partial t}(\Phi_s \rho_s) + \frac{\partial}{\partial x^i}(\Phi_s \rho_s U_s^i) = 0 \tag{1}$$

where ρ_s, Φ_s and U_s^i are, respectively, the material density, volume fraction and Favre-averaged velocity component (i-direction) of the dispersed phase which is denoted by the subscript s. The momentum equation is written as

$$\frac{\partial}{\partial t}(\Phi_s \rho_s U_s^i) + \frac{\partial}{\partial x^j}(\Phi_s \rho_s U_s^j U_s^i) = -\beta_{sf} U_r^i + \frac{\partial}{\partial x^j}(-P_s \delta^{ij} + R_s^{ij}) - \Phi_s \frac{\partial P_f}{\partial x^i} + \Phi_s \rho_s g^i \tag{2}$$

where P_f is the mean pressure field and g represents a body force per unit mass (gravity). In order to close the above equation, expressions for the particulate phase stress tensor (R_s^{ij}) and inter-phase momentum transfer term are required. Drag can be regarded as the only significant interaction force in dilute suspensions with low gas-to-particle density ratio (Lun and Savage, 2003). It can be modeled by an average drag function, β_{sf}, which takes into account

Table 1
Closure assumptions employed in this work. Additional terms can be found in (Benavides and van Wachem, 2008).

$$v_f^t = \tfrac{2}{3} k_f \tau_f^t \left[1 + c_{sf} \mathscr{X}_{sf} \eta \left(1 - \tfrac{k_{sf}}{2k_f}\right)\right]^{-1} \quad \mathscr{X}_{sf} = \tfrac{\Phi_s \rho_s}{\Phi_f \rho_f} \quad \tau_f^t = \tfrac{3}{2} c_\mu \tfrac{k_f}{\epsilon_f}$$
$$\lambda_s = \tfrac{4}{3}(1+e_s) g_0 d_s \rho_s \Phi_s^2 \sqrt{\tfrac{\Theta_s}{\pi}} \quad \mu_s = \Phi_s \rho_s \left(v_s^t + v_s^c\right) \quad \eta = \tfrac{\tau_{sf}^t}{\tau_d}$$
$$\Gamma_s = \tfrac{3}{2} \Phi_s \rho_s \left(\kappa_s^t + \kappa_s^c\right) \quad \tau_{sf}^t = \tau_f^t (1 + c_\beta \xi_r)^{-1/2} \quad \xi_r = \tfrac{3U_r^2}{2k_f}$$
$$S_s^{ij} = \tfrac{1}{2}\left(\tfrac{\partial U_s^i}{\partial x^j} + \tfrac{\partial U_s^j}{\partial x^i}\right) \quad \epsilon_s = \left(1 - e_s^2\right) \tfrac{\Theta_s}{2\tau_s^c} \quad \tau_s^c = \tfrac{d_s}{24 \Phi_s g_0} \sqrt{\tfrac{\pi}{\Theta_s}}$$
$$\beta_{sf} = \tfrac{\Phi_s \rho_s}{\tau_d} = \tfrac{3}{4} \tfrac{\Phi_s \rho_f \bar{u}_r}{d_s} C_d \quad Re_p = \tfrac{\Phi_f \bar{u}_r d_s}{v_f} \quad v_{sf}^t = \mathscr{D}_{sf}^t = \tfrac{1}{3} k_{sf} \tau_{sf}^t$$
$$\bar{u}_r \approx \sqrt{U_r^i U_r^i + \tfrac{2}{3}\left(k_f - 2k_{sf} + \tfrac{3}{2}\Theta_s\right)} \quad \mathscr{P}_{sf} = -\rho_s \left(\overline{u_f^i u_s^j} \tfrac{\partial U_s^i}{\partial x^j} + \overline{u_f^j u_s^i} \tfrac{\partial U_f^i}{\partial x^j}\right)$$
$$\overline{u_f^i u_f^j} = \tfrac{1}{3} k_f \delta^{ij} - \tfrac{2 v_f^t \eta}{1+\eta}\left(S_f^{ij} - \tfrac{1}{3} S_f^{ll} \delta^{ij}\right) - \tfrac{v_{sf}^t}{1+\eta}\left(S_{sf}^{ij} - \tfrac{1}{3} S_{sf}^{ll} \delta^{ij}\right)$$
$$\Pi_{sf} = -\beta_{sf}\left[(1 + \mathscr{X}_{sf}) k_{sf} - 3\mathscr{X}_{sf} \Theta_s - 2k_f\right] \quad \epsilon_{sf} = \tfrac{k_{sf}}{\tau_{sf}^t} \quad S_{sf}^{ij} = \tfrac{\partial U_f^i}{\partial x^j} + \tfrac{\partial U_s^j}{\partial x^i}$$

the particle concentration (Table 1). A correction coefficient suggested by Wen and Yu (van Wachem, 2000) is introduced to account for the departure from Stokes drag,

$$C_d = \begin{cases} \tfrac{24}{Re_p}\left[1 + 0.15 Re_p^{0.687}\right](1 - \Phi_s)^{-1.7} & \text{if} \quad Re_p < 1000 \\ 0.44(1 - \Phi_s)^{-1.7} & \text{if} \quad Re_p \geqslant 1000 \end{cases} \tag{3}$$

The Favre averaging of drag term leads to a dispersive force in the momentum equation. This dispersive force is included in the definition of the relative velocity, which is expressed as the difference between mean slip velocity and a drift velocity, i.e., $U_r^i = \left(U_s^i - U_f^i\right) - U_d^i$. The drift velocity, U_d^i, represents the correlation between particle velocity distribution and turbulent fluid motion at a scale larger than the particle size (Simonin, 1996). Such effect can be represented to a good approximation by a gradient-diffusion model of the form

$$U_d^i = -\mathscr{D}_{sf}^t \left(\frac{1}{\Phi_s}\frac{\partial \Phi_s}{\partial x^i} - \frac{1}{\Phi_f}\frac{\partial \Phi_f}{\partial x^i}\right) \tag{4}$$

where the turbulent dispersion coefficient, $\mathscr{D}_{sf}^t$, can be expressed as the product of a turbulence characteristic time-scale viewed by the particles and a velocity-scale determined along particle trajectories (Simonin, 1996). The particulate phase stress tensor is modeled by use of a Boussinesq assumption

$$R_s^{ij} = 2\mu_s S_s^{ij} + \left(\lambda_s - \frac{2}{3}\mu_s\right) S_s^{ll} \delta^{ij} \tag{5}$$

where transport properties are obtained from KTGF in conjunction with interstitial fluid effects, i.e., the influence of the drag and gas turbulence on the particle mean-free path (Gobin et al., 2003). An overview of closure models employed in this work is listed in Table 1. Normal forces in the dispersed phase due to particle-particle interactions are represented by the particulate phase pressure,

$$P_s = \rho_s \Phi_s \Theta_s [1 + 2(1 + e_s) g_0 \Phi_s] \tag{6}$$

Although the current investigation focuses on dilute flow in which the particle response time (τ_d) is expected to be smaller than the particle-collision time (τ_s^c), particle-particle interaction cannot be neglected completely based on the expected solids volume fraction (Crowe et al., 1996). As the derivation of closure models via KTGF assumes that the particulate phase consists of nearly elastic particles, the particle restitution coefficient (e_s) should take a value between 0.9 and 0.99. Furthermore, the sensitivity of particulate phase properties to this parameter is especially important at high concentrations (Dartevelle, 2003). As a result, this parameter is arbitrarily set to 0.95 and assumed to be equal for the three investigated particle classes.

2.1.1. Turbulence in the dispersed phase

The fluctuating motion of the dispersed phase can be quantified by the granular temperature, $\Theta_s = \frac{1}{3}\overline{u_s^i u_s^i}$, which is analogous to the thermodynamic temperature for gases (van Wachem, 2000). As the particulate phase stress tensor depends on the magnitude of particle velocity fluctuations, a balance of turbulent kinetic energy ($\frac{3}{2}\Theta_s$) is therefore needed to close the equation set. Following a two-fluid model formulation (Benavides and van Wachem, 2008) and closure assumptions from KTGF, it yields to

$$\frac{3}{2}\left[\frac{\partial}{\partial t}\left(\Phi_s \rho_s \Theta_s\right) + \frac{\partial}{\partial x^j}\left(\Phi_s \rho_s U_s^j \Theta_s\right)\right] = \left(-P_s \delta^{ij} + R_s^{ij}\right)\frac{\partial U_s^i}{\partial x^j} + \frac{\partial}{\partial x^j}\left(\Gamma_s \frac{\partial \Theta_s}{\partial x^j}\right) + \beta_{sf}(k_{sf} - 3\Theta_s) - \Phi_s \rho_s \epsilon_s \tag{7}$$

where the terms on the right hand side represent production by the mean velocity gradient, diffusion due to kinetic and collisional effects, inter-phase turbulent energy transfer and collisional rate of dissipation (ϵ_s), respectively. The inter-phase interaction term can be further split into two contributions: production of granular temperature by the gas-phase turbulence, which is represented by the correlation between fluid and particle velocity fluctuations, $k_{sf} = \overline{u_s^i u_f^i}$; and dissipation as a result of the fluctuating drag force acting on the particles (Benavides and van Wachem, 2008).

The quantity k_{sf} also requires a closure approximation. The correlation between the fluctuating motion of the gas and particulate phase needs to be determined along particle paths. As a result, modeling of the gas-particle fluctuating velocity correlation introduces the dominant role of turbulence on both the fluctuating kinetic energy and transport properties of the dispersed phase. A modeled transport equation for k_{sf} can be written as

$$\frac{\partial}{\partial t}\left(\Phi_s \rho_s k_{sf}\right) + \frac{\partial}{\partial x^j}\left(\Phi_s \rho_s U_s^j k_{sf}\right) = \Phi_s \mathscr{P}_{sf} + \frac{\partial}{\partial x^j}\left(\Phi_s \rho_s \frac{v_{sf}^t}{\sigma_k}\frac{\partial k_{sf}}{\partial x^j}\right) + \Pi_{sf} - \Phi_s \rho_s \epsilon_{sf} \tag{8}$$

where the terms on the right hand side represent production rate ($\mathscr{P}_{sf}$) due to gas and dispersed phase mean shears; turbulent transport; inter-phase interaction (Π_{sf}) which is largely determined by the particle-to-gas mass-ratio and particle inertia; and a dissipation rate that accounts for viscous and crossing-trajectory effects (ϵ_{sf}), respectively. The exact form of each term in Eq. (8) is derived from a stochastic Lagrangian description based on a generalized Langevin-type model (Haworth and Pope, 1986; Simonin, 2005), which accounts for the instantaneous slip between phase turbulent motions at moderate particle-loading ratios. Closure models are obtained by introducing a mean particle relaxation time (τ_d) determined from mean flow quantities and an average drag coefficient. Good agreement between closure assumptions based on characteristic time-scales and large-eddy simulation (LES) has been reported by Wang et al. (1998). A complete derivation of transport equations for fluid-particle velocity moments as well as closure assumptions is found in (Simonin, 1996; Simonin et al., 1993). Models for the terms on the right hand side of Eq. (8) together with characteristic time-scales and flow parameters are listed in Table 1.

2.1.2. Particulate-phase viscosity in dilute flow

A dilute dispersed phase should obey the kinetic regime, where momentum and kinetic energy transport terms are dominated by the turbulent motion. On the other hand, collisions may have a rather weak influence on the transport properties, by modifying the particle effective mean-free path. This remains an issue in gas-solid flow models, as existing models perform unsatisfactorily.

In this work, we propose a heuristic model for the particulate phase viscosity, which is formulated by following the analogy of single-phase turbulence modeling. The mechanisms of turbulence present in single-phase flow are similar to the interactions that govern turbulence in the dispersed phase - this is one of the main assumptions of KTGF. Consequently, the turbulent viscosity may be

expressed as a product of two local scalar properties, i.e. a velocity-scale ($\mathscr{U}$) and a length-scale (ℓ)

$$\nu^t \sim \mathscr{U}\ell$$

Granular temperature is an intuitive choice for a velocity-scale, $\mathscr{U} = \sqrt{\Theta_s}$, but the selection of a length-scale is not so apparent. The particle mean-free-path can be thought of as a plausible length-scale, however a characteristic length-scale of turbulent gas-particle flow needs to account for eddy-particle interaction. As a result, the turbulent length-scale viewed by a particle is chosen as a representative length dimension, i.e.

$$\ell^t = c_L \frac{k_f^{3/2}}{\epsilon_f}(1 + c_\beta \xi_r)^{-1/2}$$

where the parameter ξ_r aims at modeling the relative velocity between particles and eddy structures, which is known as the crossing-trajectory effect (Simonin et al., 1993). Furthermore, the particle mean-free path can be employed to impose a limit on the particulate phase length-scale

$$\ell_{mfp} = \frac{d_s/\Phi_s}{6\sqrt{2}}$$

So the turbulent characteristic length of the dispersed phase is determined from

$$\ell_s = \min(\ell^t, \ell_{mfp})$$

and the shear viscosity that appears in the the particulate phase stress tensor Eq. (5) can be finally written as

$$\mu_s = \Phi_s \rho_s \ell_s \sqrt{\Theta_s} \tag{9}$$

Analogously, a closure model for the particulate phase conductivity in Eq. (7) can be expressed as

$$\Gamma_s = \frac{3}{2}\frac{\mu_s}{\sigma_\theta} \tag{10}$$

2.2. Gas phase

Total volume conservation requires that $\Phi_s + \Phi_f = 1$. As a result, a differential form can be obtained by adding the continuity equations for the gas and dispersed phase. It yields to

$$\frac{\partial}{\partial x^i}\left[\Phi_s U_s^i + (1-\Phi_s)U_f^i\right] = 0 \tag{11}$$

A discretized form of Eq. (11) is therefore used to determine a pressure-correction equation (Vasquez and Ivanov, 2000). Momentum balance is analogous to Eq. (2)

$$\frac{\partial}{\partial t}\left(\Phi_f \rho_f U_f^i\right) + \frac{\partial}{\partial x^j}\left(\Phi_f \rho_f U_f^j U_f^i\right) = \frac{\partial}{\partial x^j}\left[\Phi_f\left(\mathscr{T}_f^{ij} + R_f^{ij}\right)\right] - \Phi_f \frac{\partial P_f}{\partial x^i} + \beta_{sf} U_r^i \tag{12}$$

where $\mathscr{T}_f^{ij}$ is the viscous stress tensor, i.e. a Newtonian fluid. An eddy-viscosity assumption is used to model the Reynolds stress tensor, R_f^{ij}, generalized to gas-particle flow by use of a modified eddy-viscosity (ν_f^t) provided in Table 1

$$R_f^{ij} = 2\rho_f \nu_f^t\left(S_f^{ij} - \frac{1}{3}S_f^{ll}\delta^{ij}\right) - \frac{2}{3}\rho_f k_f \tag{13}$$

where S_f^{ij} is analogous to S_s^{ij} in Table 1.

2.2.1. Turbulence transport equation

A two-equation model is employed to account for turbulence in the carrier phase, being turbulence modulation the most distinctive model adjustment. A transport equation for turbulent kinetic energy can be written as

Table 2
$k-\epsilon$ dispersed turbulence model coefficients.

c_μ	$c_{\epsilon 1}$	$c_{\epsilon 2}$	$c_{\epsilon 3}$	σ_k	σ_ϵ	σ_θ	c_L	c_{sf}	c_β
0.09	1.44	1.92	1.2	1.0	1.3	0.72	$\sqrt{\frac{3}{2}c_\mu}$	0.34	$1.8 - 1.35\cos^2\theta$

$$\frac{\partial}{\partial t}(\Phi_f \rho_f k_f) + \frac{\partial}{\partial x^j}(\Phi_f \rho_f U_f^j k_f) = \frac{\partial}{\partial x^j}\left(\Phi_f \rho_f \frac{\nu_f^t}{\sigma_k}\frac{\partial k_f}{\partial x^j}\right) + \Phi_f \mathscr{P}_{k_f} - \Phi_f \rho_f \epsilon_f + \Pi_{k_f} \tag{14}$$

where the term $\mathscr{P}_{k_f}$ stands for production of turbulent kinetic energy from the mean flow. An analogous equation for the rate of dissipation, ϵ_f, is given by

$$\frac{\partial}{\partial t}(\Phi_f \rho_f \epsilon_f) + \frac{\partial}{\partial x^j}\left(\Phi_f \rho_f U_f^j \epsilon_f\right) = \frac{\partial}{\partial x^j}\left(\Phi_f \rho_f \frac{\nu_f^t}{\sigma_\epsilon}\frac{\partial \epsilon_f}{\partial x^j}\right) + \frac{\epsilon_f}{k_f}\left(c_{\epsilon 1}\Phi_f \mathscr{P}_{k_f} - c_{\epsilon 2}\Phi_f \rho_f \epsilon_f + c_{\epsilon 3}\Pi_{k_f}\right) \tag{15}$$

The term Π_{k_f} in Eqs. (14 and 15) accounts for turbulence modification by the presence of particles

$$\Pi_{k_f} = -\beta_{sf}\left(2k_f - k_{sf} - U_r^i U_d^i\right) \tag{16}$$

The above term may lead to attenuation of gas turbulence as particle mass-loading ratio is increased (Gobin et al., 2003). The first two terms between parenthesis are responsible for dissipation by drag and energy transfer to particulate phase fluctuations, respectively; the last term modulates turbulent kinetic energy as a result of turbulent particle transport, although its contribution is expected to be very small (Simonin, 1996). Finally, the employed turbulence model coefficients are listed in Table 2. Coefficient c_β depends on the angle (θ) between dispersed phase mean velocity and mean relative velocity.

3. Numerical procedure

The computational domain consists of a two-dimensional channel section which starts $65h$ upstream from the step and extends up to $34H$ downstream, as it is illustrated in Fig. 1. A coordinate system is located at the step with the x axis parallel to the channel wall. Gas and particulate phase properties, such as the material density, laminar viscosity and particle diameter are set to constant values, e.g. the gas-phase is air at standard conditions.

The commercial CFD software Fluent 6.3 is used to solve the Eulerian-Eulerian equations of incompressible two-phase flow. Built-in transport properties of the particulate phase do not account for the influence of an interstitial fluid, i.e. models from kinetic theory of dry granular flow are the default option (Gidaspow, 1994). Implementation of the closure assumptions summarized in Table 1, Eqs. (9 and 10), and inter-phase momentum and kinetic energy transfer terms is carried out via user-defined function (UDF) subroutines. Similarly, the UDF capability allows to incorporate the transport equation for k_{sf} which is the major code development in the current work.

All the governing equations for both gas and dispersed phase are solved sequentially at each iteration. Third-order upwind difference for the convective term in Eqs. (1, 2, 7, 8, 12, 14 and 15), and second-order central difference for other terms are used. The time-step is set to 10^{-4} s. Momentum equations are solved followed by total volume continuity and velocity updates. Transport equations for turbulence are subsequently solved by use of the updated velocity field. Properties, such as the eddy-viscosity and particulate phase pressure are updated which are then used in the

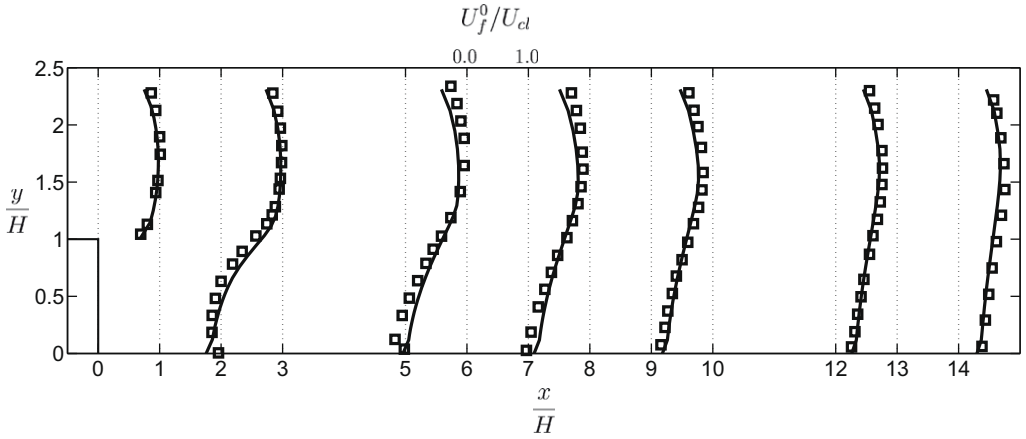

Fig. 2. Normalized stream-wise gas mean velocity. Open symbols represent the experiment of Fessler and Eaton (1995) for unladen flow and curves are numerical predictions for single phase (U_f^0). The center-line velocity (U_{cl}) is 10.5 m/s.

Table 3
Detailed description of simulated cases.

	d_s (μm)	ρ_s (kg/m^3)	Loading	τ_d (ms)	St	Re_p
Case 1	150	2500	20% and 40%	101	7.9	10.1
Case 2	90	2500	20%	48	3.8	2.9
Case 3	70	8800	10% and 40%	94.5	7.4	4.4

momentum equations for the next time-step. The solution process is marched towards a steady-state and is repeated until a converged solution is obtained.

3.1. Boundary conditions

In order to attain a center-line velocity (U_{cl}) of about 10.5 m/s at the step ($x/H = 0$), a uniform velocity (U_{in}) of 9.3 m/s is specified at the channel inlet, which corresponds to a Reynolds number ($Re_{h/2}$) of 1.3×10^4. This figure is estimated from the reported experimental measurements of stream-wise mean velocity along the test section (Fessler and Eaton, 1995). A turbulence intensity of 1% and channel half-width ($h/2$) as the representative turbulence length-scale are also specified. In order to match a specific particle mass-loading, a uniform particulate phase volume fraction (Φ_s) is specified at the inlet, which is calculated by assuming a constant particle-to-gas velocity ratio. No appreciable influence of the particulate phase velocity inlet condition has been observed on the simulation results. In fact, an indistinguishable fully-developed gas-particle flow field is obtained along the channel section ($x/H < 0$) as long as the loading is satisfied.

A standard-wall function treatment is employed at the wall for the gas-phase mean velocity and turbulence quantities. Wall adjacent nodes are therefore placed in the logarithmic layer and the influence of particles on the law of the wall is not considered. Regarding the dispersed phase, the particulate phase shear stress is set equal to the momentum flux transferred to the wall as a result of particle-wall collisions (Johnson and Jackson, 1987). Likewise, a wall-boundary condition for the granular temperature is derived from an energy balance on a thin region adjacent to the wall (Benavides and van Wachem, 2008). As a first approximation, zero normal-gradient condition is applied to k_{sf} at the wall.

Derivatives of velocity components, particulate phase volume fraction and turbulent quantities are set to zero at the outlet as the flow is expected to be fully-developed.

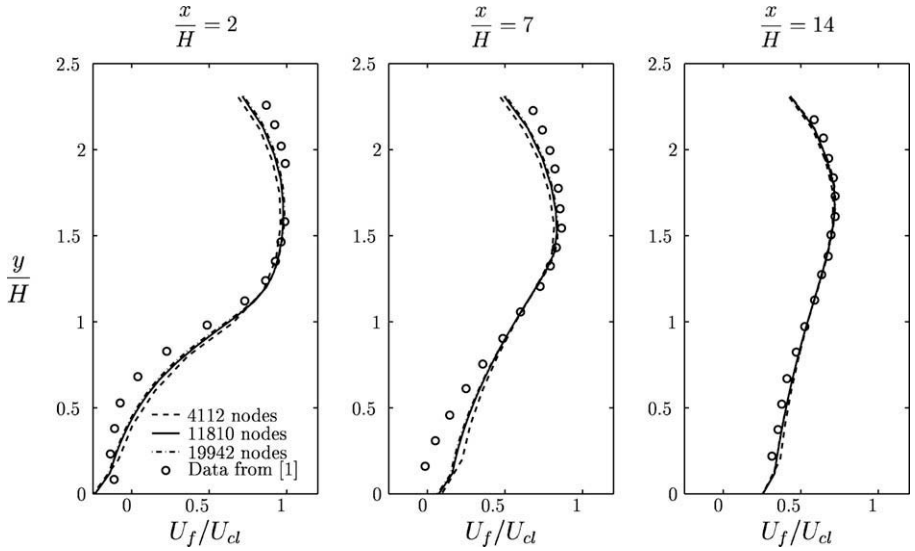

Fig. 3. Grid-independent solutions of stream-wise gas-phase mean velocity in the presence of 70 μm copper particles (Case 3). The particle mass-loading is 40%.

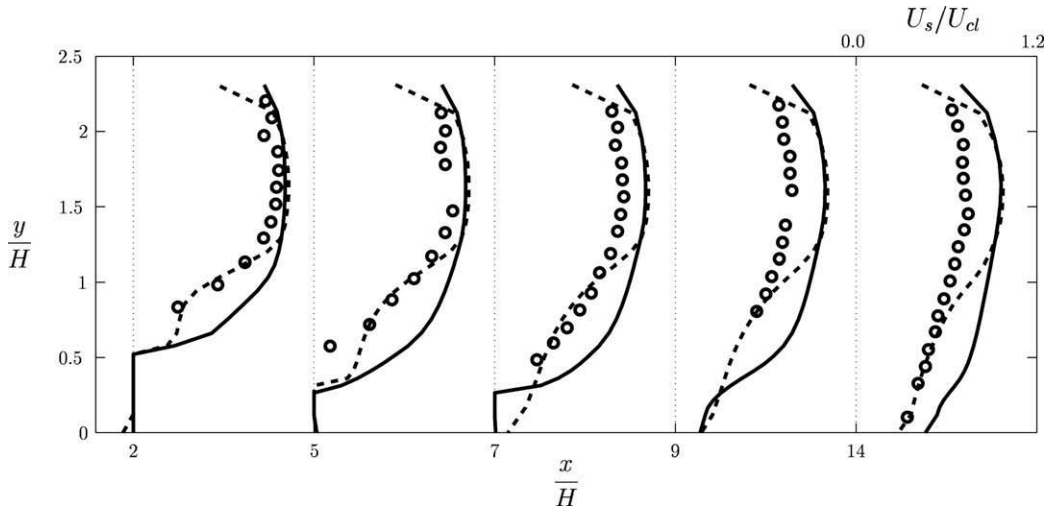

Fig. 4. Stream-wise particulate phase mean velocity for Case 1. Solid line: dispersed phase viscosity model Eq. (9); dashed line: KTGF. Open symbols represent experimental data for particle mass-loading of 40%, (Fessler and Eaton, 1995).

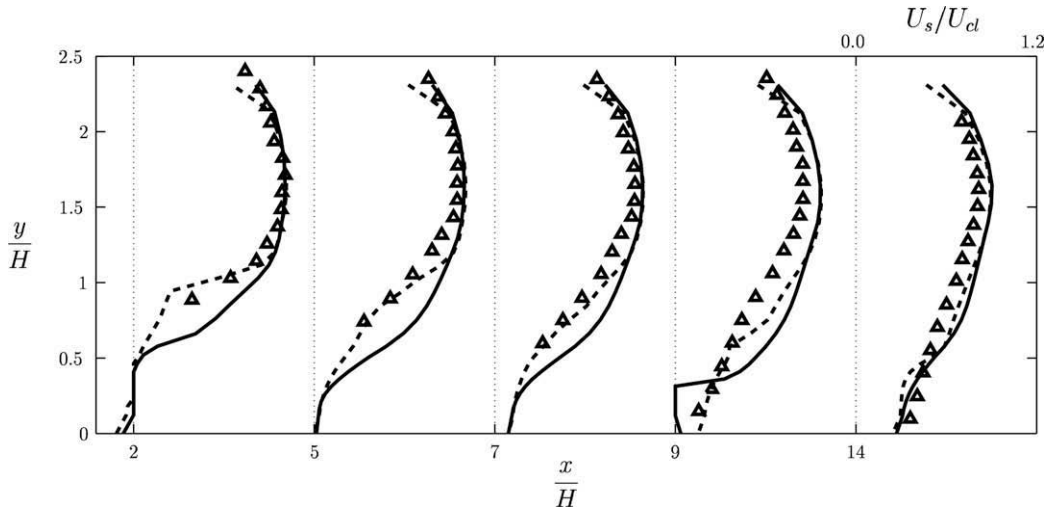

Fig. 5. Stream-wise particulate phase mean velocity for Case 2. Solid line: dispersed phase viscosity model Eq. (9); dashed line: KTGF. Open symbols represent experimental data for particle mass-loading of 20%, (Fessler and Eaton, 1995).

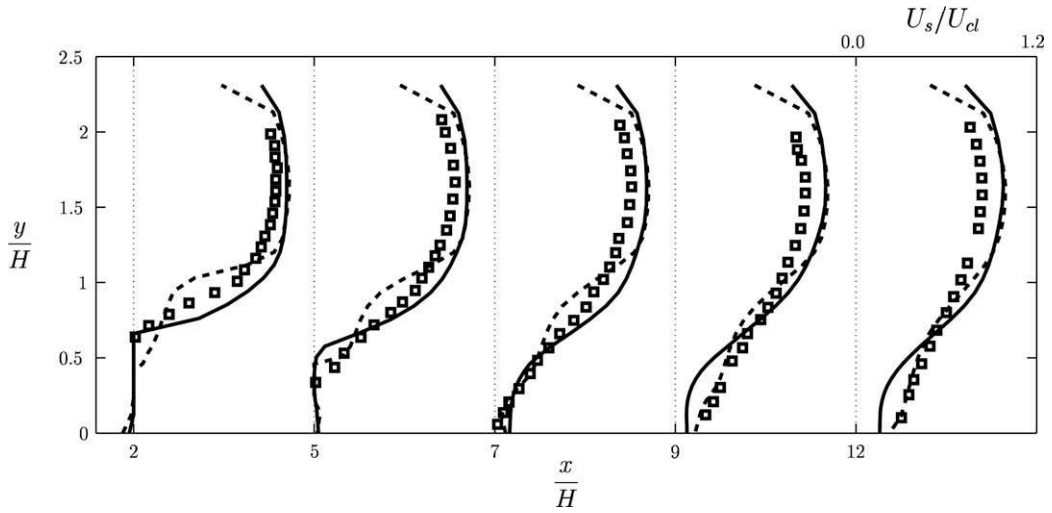

Fig. 6. Stream-wise mean velocity for Case 3. Solid line: dispersed phase viscosity model Eq. (9); dashed line: KTGF. Open symbols represent the experimental data for mass-loading of 10%, (Fessler and Eaton, 1999).

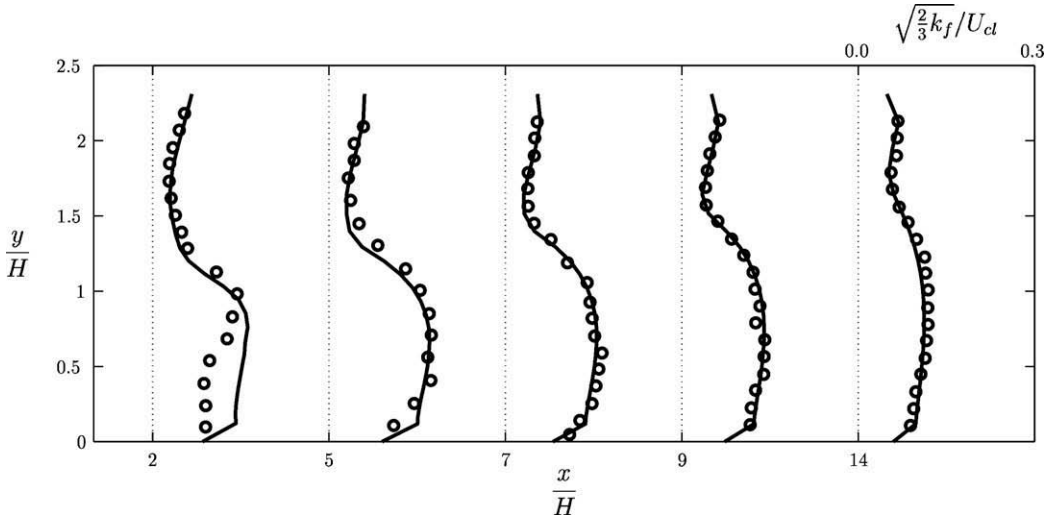

Fig. 7. Turbulence intensity profiles for Case 1. Open symbols represent measurements of stream-wise gas-phase fluctuating velocity in the presence of 150 μm glass particles with mass-loading of 40%, (Fessler and Eaton, 1999).

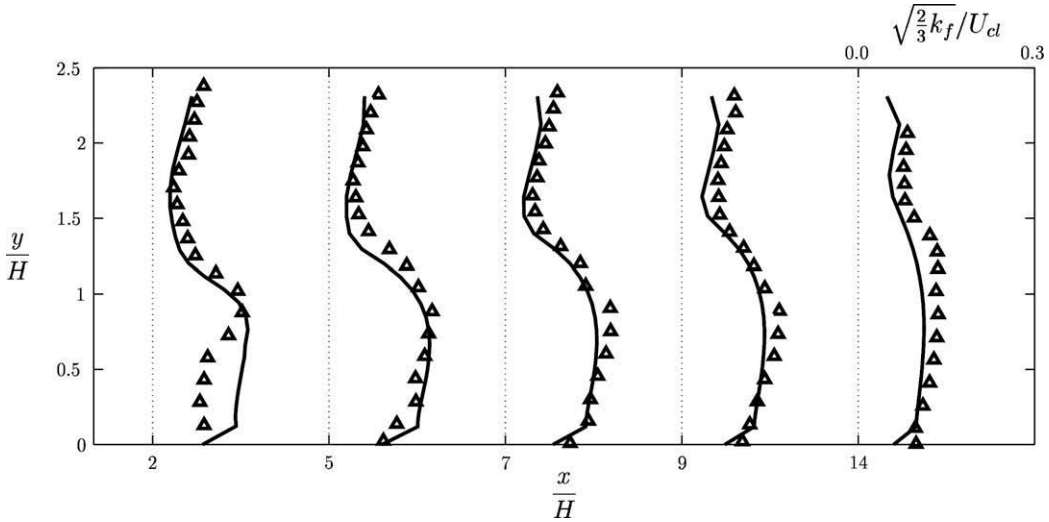

Fig. 8. Turbulence intensity profiles for Case 2. Open symbols represent measurements of stream-wise gas-phase fluctuating velocity in the presence of 90 μm glass particles with mass-loading of 20%, (Fessler and Eaton, 1999).

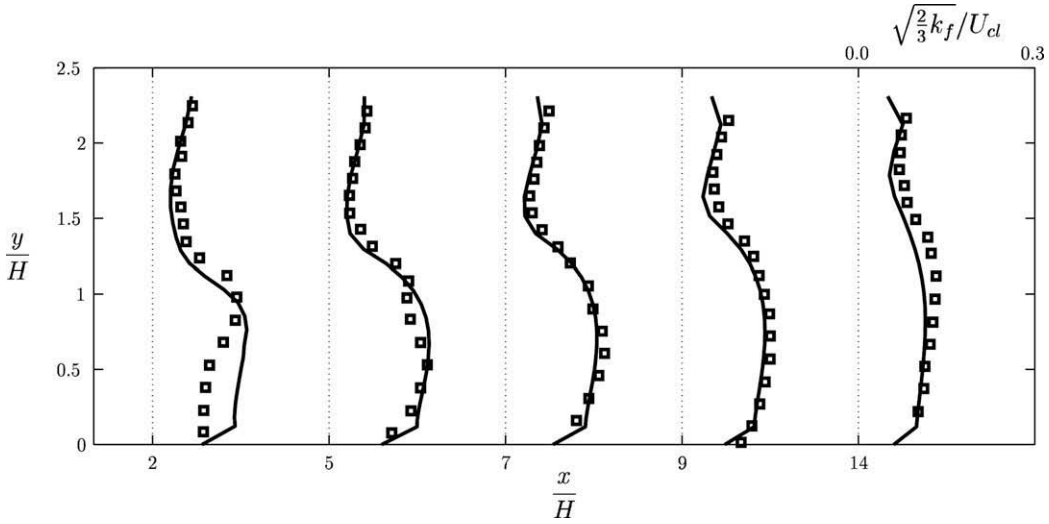

Fig. 9. Turbulence intensity profiles for Case 3. Open symbols represent measurements of stream-wise gas-phase fluctuating velocity in the presence of 70 μm copper particles with mass-loading of 40%, (Fessler and Eaton, 1999).

4. Results and discussion

Attention is devoted to the comparison of mean quantities of both the gas and dispersed phases, especially the particulate phase mean velocity and turbulence intensity of the gas. The simulated results from the Eulerian two-fluid model are compared against the benchmark experimental data of Fessler and Eaton (1995), Fessler and Eaton (1999). For example, Fig. 2 shows the comparison of the detailed gas flow field with benchmark experimental data for single-phase flow (Fessler and Eaton, 1995). Velocity profiles are given at several downstream positions of which the recirculation $(x/H = 2)$, reattachment $(x/H = 7)$, and redevelopment $(x/H = 14)$ positions are of particular interest.

The present numerical investigation focuses on three distinctive particle classes. The simulated cases are listed in Table 3. The particulate phase in Case 1 and 2 consists of the same material (glass) whereas particle diameter (d_s) and mass-loading are varied. The particle response time is calculated by use of Eq. (3) for a single particle. A fluid time-scale based on an approximate large-eddy passing frequency is used to estimate the particle Stokes number (St) i.e.

$$St = \frac{\tau_d U_{cl}}{5H} \tag{17}$$

The flow in Case 3 carries copper particles. Results from 10% mass-loading are chosen to evaluate the grid dependence of the computations. Stream-wise gas-phase mean velocity profiles are shown in Fig. 3. Particle laden flow calculations are conducted with three types of grid systems. The presented results may acknowledge a grid-independent solution in the calculations as the two finest grids have yielded almost identical velocity profiles that are in reasonable

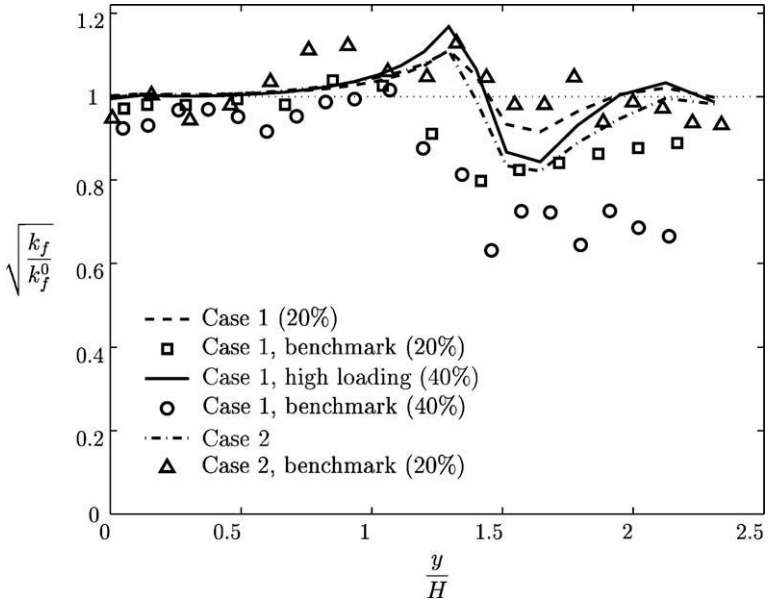

Fig. 10. Predictions of turbulence modulation by 90 μm and 150 μm glass particles at $x/H = 7$. Benchmark data from (Fessler and Eaton, 1999).

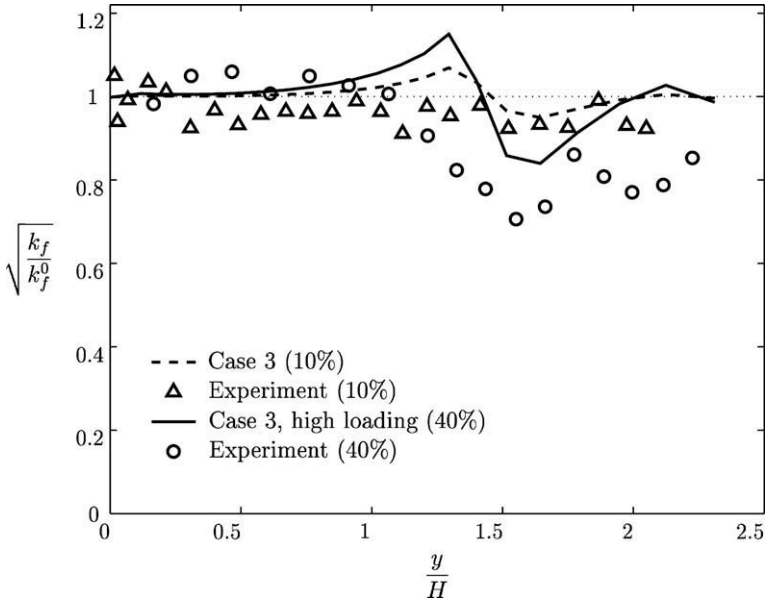

Fig. 11. Predictions of turbulence modulation by 70 μm copper particles at $x/H = 7$. Benchmark data from (Fessler and Eaton, 1999).

agreement with the benchmark data (Fessler and Eaton, 1999). Hence, a grid resolution of 11,810 nodes (Fig. 3) is employed to perform subsequent numerical simulations. Such grid consists of 26 nodes in the transverse direction and 228 nodes in the stream-wise x-direction past the step. The average grid spacing is estimated to be 3.8 mm, whereas wall adjacent nodes are placed at 5 mm.

Results of stream-wise particulate phase mean velocity are validated for all particle classes. Two sets of numerical results for the particulate phase are obtained by using closure relations from KTGF for the shear viscosity and diffusivity, and the derived model given by Eqs. (9 and 10). Figs. 4 and 6 show velocity profiles for particles with comparable Stokes number. Profiles at the reattachment and redevelopment regions indicate that the dispersed phase mean velocity is somewhat overestimated ($y/H > 1$) in the case of massive particles. Such discrepancy may be due to the assumption of uniform particle size distribution, as particles with a relatively large Stokes number are less responsive to the gas-phase flow field. Furthermore, the new shear viscosity model evidently overestimates the stream-wise mean velocity in the case of high particle Reynolds number (Case 1). On the other hand, Fig. 5 shows a better agreement between model predictions and experimental data in the case of light particles (i.e. Case 2, see Table 3) which exhibit a rather low slip, as it is indicated by the particle Reynolds number. In general, closure relations from KTGF give a better prediction of the particulate phase mean velocity.

Stream-wise gas turbulence intensity profiles are plotted in Figs. 7–9 for the three simulated cases at several downstream positions. There is fair agreement between the simulation predictions and the experimental measurements for the three cases. Turbulence intensity is over-predicted in the recirculation region as a result of the inherent isotropic nature of the $k-\epsilon$ model. The choice of particulate phase shear viscosity model is not found to have a significant influence on the gas turbulent kinetic energy.

The effect of particles on the gas turbulence is further examined by looking at the ratio of the turbulent kinetic energy for particle-laden flow to that of the single-phase flow (k_f^0) at the reattachment region ($x/H = 7$). It is shown in Fig. 10 that the model is able to account for turbulence modification with increasing particle mass-

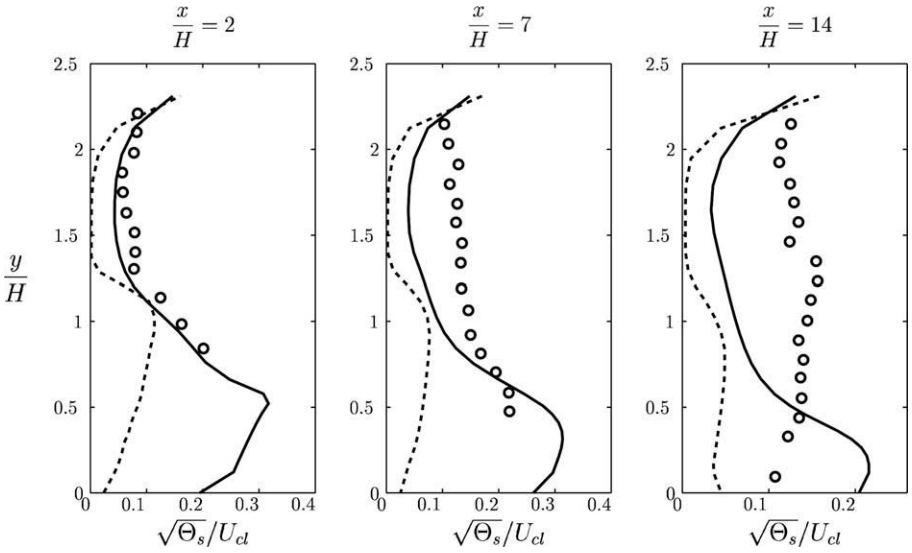

Fig. 12. Turbulence intensity in the particulate phase. Solid line: dispersed phase viscosity model Eq. (9); dashed line: KTGF. Open symbols represent measurements of particle stream-wise fluctuating velocity for Case 1 with mass-loading of 40%, (Fessler and Eaton, 1995).

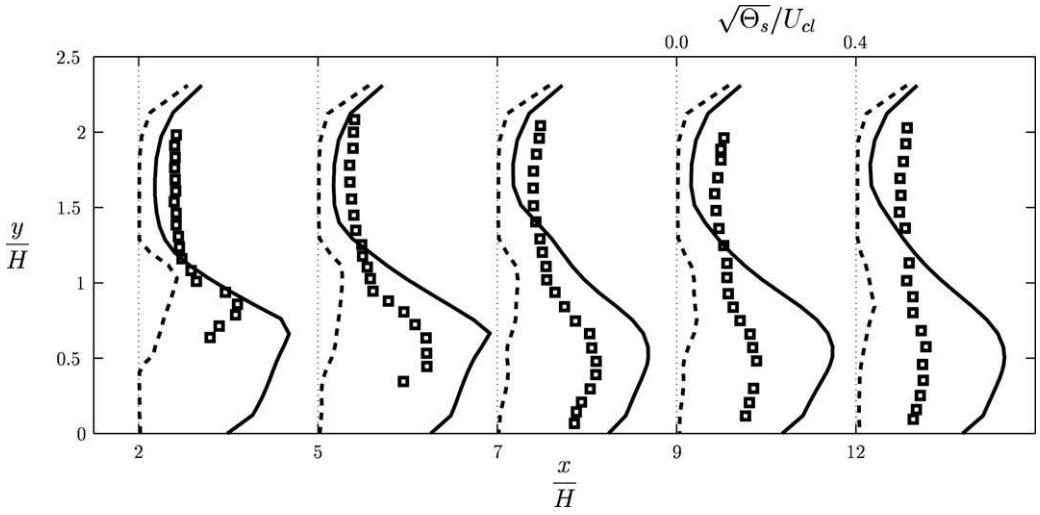

Fig. 13. Turbulence intensity in the particulate phase. Solid line: dispersed phase viscosity model Eq. (9); dashed line: KTGF. Open symbols represent measurements of particle stream-wise fluctuating velocity for Case 3 with mass-loading of 10%, (Fessler and Eaton, 1999).

loading (Case 1). However, the turbulence attenuation is evidently under-estimated at $y/H > 1$. In addition, the model erroneously predicts turbulence enhancement at about $y/H = 1.4$. Fig. 11 shows a similar trend on turbulence modulation by copper particles (Case 3), where significant attenuation is found at $y/H > 1$.

Finally, predictions of particulate phase turbulence intensity are compared with experimental measurements of particle stream-wise fluctuating velocity. Figs. 12 and 13 clearly show that particle fluctuations along the channel are under estimated when KTGF models are employed. On the other hand, it can be argued that the new shear viscosity model given by Eq. (9) results in a minor improvement in the prediction of turbulence intensity. It is found that the new model increases the production of particulate phase turbulent kinetic energy from the mean flow. There is good agreement at the recirculation region, however the predicted turbulence intensity remains nearly unmodified at subsequent downstream positions.

5. Conclusions

An Eulerian-based computational study of a vertically oriented backward-facing step with turbulent gas-particle flow has been performed. A *four-equation model* for turbulent gas-particle flow is derived and validated in this work. A balance equation for the turbulent kinetic energy associated with particle velocity fluctuations together with a transport equation for the gas-particle fluctuating velocity correlation are employed to model turbulence in the dispersed phase. A novel particulate phase shear viscosity model is presented, derived analogously to single-phase turbulence modeling. An extension of the k-ϵ model for a single-phase to the case of two-phase flow is used to account for turbulence in the carrier gas-phase. In addition, inter-phase turbulent kinetic energy transfer terms are incorporated to account for two important flow characteristics: particle transport by fluid-turbulence and turbulence modulation.

The resulting model is used to simulate turbulent air flow loaded with three different types of particles and mass-loading conditions. Numerical predictions of gas and particulate phase stream-wise mean velocity and turbulence intensity at various downstream positions are compared to experimental data. In general, calculations are found to be in reasonable agreement with the benchmark experimental data (Fessler and Eaton, 1995; Fessler and Eaton, 1999), and there is fairly good qualitative agreement with turbulence modulation results. The new model for the particulate phase shear viscosity, which considers the crossing-trajectory effect, is able to capture the particle fluctuating velocity profiles more correctly than previous KTGF models.

The current work demonstrates that the presence of a dispersed phase has a significant effect on the gas-phase fluctuating and mean velocity field, even at a relatively low particulate phase volume fraction. Moreover, inter-phase interactions at the level of turbulent fluctuations may influence not only the turbulent kinetic energy distribution, but also the gas and particulate phase mean velocity field. Despite the overall improvement of the model predictions for dilute turbulent gas-particle flow, small discrepancies still exist which should be investigated further.

Acknowledgement

This project is funded by STEM (Energimyndigheten). Computer time provided by C^{3}SE is gratefully acknowledged.

References

Benavides, A., van Wachem, B., 2008. Numerical simulation and validation of dilute turbulent gas-particle flow with inelastic collisions and turbulence modulation. Powder Technol. 182 (2), 294–306.

Crowe, C., Troutt, T., Chung, J., 1996. Numerical models for two-phase turbulent flows. Annu. Rev. Fluid Mech. 28, 11–43.

Dartevelle, S. 2003. Numerical and granulometric approaches to geophysical granular flows, PhD thesis, Department of Geological and Mining Engineering, Michigan Technological University, Houghton, Michigan.

Elgobashi, S., 1994. On Predicting Particle-Laden Turbulent Flows. Appl. Sci. Res. 52, 309–329.

Fessler, J., Eaton, J., 1995. Particle-turbulence interaction in a backward-facing step flow, Rep. MD-70, Mech. Engng Dept. Stanford University, Stanford, California.

Fessler, J., Eaton, J., 1999. Turbulence modification by particles in a backward-facing step flow. J. Fluid Mech. 394, 97–117.

Gidaspow, D., 1994. Multiphase Flow and Fluidization: Continuum and Kinetic Theory Descriptions. Academic Press, San Diego, California.

Gobin, A., Neau, H., Simonin, O., Llinas, J., 2003. Fluid dynamic numerical simulation of a gas phase polymerization reactor. Int. J. Numer. Meth. Fluids 43, 1199–1220.

Hadinoto, K., Curtis, J., 2004. Effect of interstitial fluid on particle-particle interactions in kinetic theory approach of dilute turbulent fluid-particle flow. I & EC Research 43, 3604–3615.

Haworth, D., Pope, S., 1986. A generalized Langevin model for turbulent flows. Phys. Fluids 29, 387–405.

Johnson, P., Jackson, R., 1987. Frictional–collisional constitutive relations for granular materials, with application to plane shearing. J. Fluid Mech. 176, 67–93.

Lun, C., 2000. Numerical simulation of dilute turbulent gas-solid flows. Int. J. Multiphase Flow 26, 1707–1736.

Lun, C., Savage, S., 2003. Kinetic Theory for Inertia Flows of Dilute Turbulent Gas-Solids Mixtures. In: Lecture Notes in Physics: Theory of Granular Gases. Springer, New York.

Lun, C., Savage, S., Jeffrey, D., Chepurniy, N., 1984. Kinetic theories for granular flow: inelastic particles in Couette flow and slightly inelastic particles in a general flowfield. J. Fluid Mech. 140, 223–256.

Simonin, O. 1996. Continuum modelling of dispersed turbulent two-phase flows, Lecture series 1996-02, Laboratoire National d'Hydraulique - EDF 6 Quai Watier - 78400 Chatou/France.

Simonin, O. 2005. Statistical and Continuum Modelling of Turbulent Reactive Particulate Flows. Part I: Theoretical Derivation of Dispersed Phase Eulerian Modelling from Probability Density Function Kinetic Equation, Lecture series 2005-04, Département MFTT - EDF 6 Quai Watier, 78400 Chatou/France.

Simonin, O., Deutsch, E., Minier, J., 1993. Eulerian Prediction of the Fluid/Particle Correlated Motion in Turbulent Two-Phase Flows. Appl. Sci. Res. 51, 275–283.

van Wachem, B. 2000. Derivation, implementation and validation of computer simulation models for gas-solid fluidized beds, Dissertation, Delft University of Technology, Delft, The Netherlands.

Vasquez, S., Ivanov, V. 2000. A phase coupled method for solving multiphase problems on unstructured meshes, Proceedings of ASME FEDSM 2000, ASME 2000 Fluids Engineering Division Summer Meeting, 11-15 June, Boston, Massachusetts.

Wang, Q., Squires, K., Simonin, O., 1998. Large eddy simulation of turbulent gas-solid flows in a vertical channel and evaluation of second-order models. Int. J. Heat Fluid Flow 19, 505–511.

Yu, K., Lau, K., Chan, C., 2004. Numerical simulation of gas-particle flow in a single-side backward-facing step flow. J. Comput. Appl. Math. 163, 319–331.

Zhang, Y., Reese, J., 2003. Gas turbulence modulation in a two-fluid model for gas-solid flows. AIChE J. 49, 3048–3065.